Surfaces and Interfaces 9 (2017) 218–227

Contents lists available at ScienceDirect

Surfaces and Interfaces

journal homepage: www.elsevier.com/locate/surfin

Optimization the electrophoretic deposition fabrication of graphene-based electrode to consider electro-optical applications

Sepehr Lajevardi Esfahani[a], Shohre Rouhani[a,c,*], Zahra Ranjbar[b,c]

[a] Organic colorants department, Institute for color science and technology (ICST), Tehran, Iran
[b] Organic coatings and novel technologies, Institute for color science and technology (ICST), Tehran, Iran
[c] Center of excellence for color science and technologies, Institute for color science and technology (CECST), Tehran, Iran

ARTICLE INFO

Keywords:
Electrophoretic deposition (EPD)
Graphene oxide (GO)
Electrical conductivity
Electro-optical devices

ABSTRACT

In this study, the optimized conditions of electrophoretic deposition (application potential, application time and concentration of stable graphene oxide (GO) suspension) for development of ultra-thin graphene film on copper substrate are introduced. The current density and deposition efficiency analysis, Ohm resistance measurement, SEM, FTIR and AFM techniques were done on prepared samples. The electrical conductivity of graphene coated copper substrate was increased three times more than bare copper. All of the carried tests showed that by increasing the key parameters of EPD, the average thickness of electrodeposited GO layers are increased continually so that the GO concentration effect is the most evident factor. The minimum sheet resistance and average thickness of electrodeposited RGO layers with uniform wrinkled morphology are achieved at EPD conditions of 2 V in 10 s and annealed at 200 °C for 1 min. The results of this research manifested that the EPD technique is a promising route to a low cost and well controllable method to fabricate a very conductive electrode base for electro-optical devices.

1. Introduction

Graphene with unique electrical, optical and mechanical properties has been used for many aspects of electro-optical devices [1,2].

Major graphene synthesis methods are described with detailed information regarding process parameters and graphene characteristics. Among various synthesis techniques, emphasis is given on mechanical exfoliation, chemical vapor deposition, chemical synthesis, and epitaxial growth as the most popular graphene synthesis methods among scientists and researchers. Other important issues of graphene synthesis, such as fabrication of functionalized graphene, large-scale graphene growth and graphene transfer onto other substrates, have also been summarized [3].

Depending on the chemical structure and properties of graphene, it is produced in different methods [3,4]. Graphene has many advantages due to quantum effects of a single atomic layer or few atomic layers [5]. Graphene oxide can be reduced via using different methods [5,6]. Due to the difference in the conductivity of reduced graphene oxide and graphene oxide, an easy and efficient way to deploy reduced graphene oxide is required in many applications [7–9].

Electrophoretic deposition method (EPD) is used for applying graphene and graphene-based nano materials for a wide range of applications, including materials for energy storage [10], fuel cells, solar cells [11], super capacitors and sensors [12]. This type of carbon nano material can be dispersed in organic solvents mainly in water [13,14].

Most materials are electrophoretically applied under constant electrical potential in different application times [15]. These two parameters (electrical potential and time of application) play an important role in the morphology of created nano material layers [16].

In addition to the simple plannar substrates, researches have shown that graphene can intract on the basis of uniform layers on complex three-dimontional substrates, porous and flexible substrates through EPD method [17–19]. In general, the graphene layers applied by EPD show that excellent properties, for example, high electrical conductivity, large surface area, good thermal stability, high optical transparency and appropriate mechanical strength [20–23]. Also, the composites contain graphene are applicable very well by EPD, for example, graphene with metallic nano particles or carbon combined with other materials like carbon nano tubes (CNT) [24,25].

Given the importance of using a highly conductive substrate with a facile manufacturing process in electro-optical devices, graphene as an appropriate material is known in this field [26–29].

In various investigations, formation of graphene layers by EPD

* Corresponding author.
E-mail address: rouhani@icrc.ac.ir (S. Rouhani).

http://dx.doi.org/10.1016/j.surfin.2017.10.001
Received 28 July 2017; Received in revised form 25 September 2017; Accepted 8 October 2017
Available online 09 October 2017

method introduced but optimization of all parameters involved in the process of electrophoretic depositing of graphene to ensure all electrical and optical properties suitable for electro-optical applications not yet fully paid. In this study we have tried to meet this challenge to be addressed more fully.

Although several studies have investigated on the EPD of GO, the key parameter's effect of EPD process on thickness and conductivity of uniform film not investigated completely.

In this research work, anodic electrodeposition of stable graphene oxide suspension was done on bare copper foil. The key parameters of EPD process (concentration of GO suspension, electrical potential and application time) due to the better morphology and electrical conductivity and minimum thickness of electrodeposited GO layers were optimized.

2. Experimental

2.1. Materials

The used materials (with their suppliers) are included of graphene oxide nano-platelets (Nanosany Co.), $Mg(NO_3)_2$, NaOH, Methoxy ethanol (Merck Co.) and Copper foil #40 μm (SDK-Metal Co.).

The analytical grade of graphene oxide nano-platelets with the characteristics shown in Table 1 was used.

2.1.1. Testing methods and equipments

The characteristics of used equipments in this research work are listed in Table 2.

2.1.2. Stabilization of GO suspension

First, the stable suspension of 0.2 (%w/w) GO in distilled water was prepared through ultra-sonication process (@ 35 Hz / 40 °C /for 2 h) [30]. In these conditions, the suspension was completely stable for 6 month and the pH of suspension was 2.7 at 23 °C. The stable GO suspension image after ultra-sonication process is shown in Fig. 1.

The stable GO suspension was divided into two parts so that the concentration of first part was 0.2 (w/w) GO in distilled water (the prepared samples with codes of: 0.2G-210, 0.2G-220, 0.2G-510, 0.2G-520) and the concentration of second part was 0.01 (w/w) (the prepared samples with codes of: 0.01G-210, 0.01G-220, 0.01G-510, 0.01G-520). The two parts were then mixed with 4 mL of Methoxy ethanol and 0.5 mL of 5% (w/w) NaOH in distilled water. In this condition the pH of stable suspension was 7.7. Therefore, these stable suspensions were suitable for anodic electrophoretic deposition.

2.1.3. Electrophoretic deposition process

For anodic electrophoretic deposition process of GO suspension, the copper foil (~40 μm in 2 * 8 cm diameters and treated with Isopropyl alcohol) and graphite rod were used as anode and cathode respectively. The distance between anode and cathode was 5.0 cm and anode to cathode area ratio was 3.3. The temperature of electrophoretic bath was kept at 25 °C for all of the samples. The anodic electrophoretic deposition process of GO is shown in Fig. 2.

For optimization the electrophoretic conditions of GO deposition on Cu substrate (GO concentration, application potential, application time and thermal annealing) the conditions shown in Table 3 were

Table 1
The characteristics of graphene oxide nano-platelets.

Purity	99.5%
Thickness of formed layers on the substrate	2–18 nm
pH (for application conditions)	7–7.7
Volume resistance	4×10^{-4} Ohm.cm
particle size	4–12 μm
Carbon & Oxygen contents	C = 92.7%, O ≤ 7.3%

Table 2
The characteristics of used equipments.

Equipment	Model
Digital balance (with accuracy of 0.01 mg)	Sartorius/ CPA 2245
Ultra-sonicator	Bandelin electronic/ 510 h
Rectifier	Wachter/ 0–600 V, 0–15 A
Aven	Carbolite/ CSF1100
Ohm meter	Fluke/ 1550B
FTIR	Perkin Elmer/ Spectrum-one
Scanning electron microscope (SEM)	LEO 1455 VP
UV–Vis absorption spectrophotometer	CECIL CE9200
X-ray diffractometer	Bruker AXSD-8 Advance X-ray diffractometer (monochromatic CuKα radiation (λ = 1.5406 A°) with scan rate of 0.1° min^{-1})
Raman spectroscope	Horiba Jobin Yvon (at λ = 532 nm laser power 1.7 mW, 100 x objective lens, 0.9 NA)
Atomic force microscope (AFM)	Micro Photonics Inc/ Dual scope DS 95–200E

Fig. 1. The stable GO suspension after ultra-sonication process.

Fig. 2. The anodic electrophoretic deposition process of GO on Cu foil.

Table 3
Electrophoretic conditions of GO deposition on Cu substrate.

Run	GO conc. (% w/w)	Application voltage (V)	Application time (s)	Thermal annealing	Initial visually result
1.	0.01	2	10	1 min @ 200 °C	Appropriate
2.	0.01	2	20	1 min @ 200 °C	Appropriate
3.	0.01	2	10	1 min @ 400 °C	Weakly adhesion
4.	0.01	2	20	1 min @ 400 °C	Weakly adhesion
5.	0.01	2	10	1 min @ 600 °C	Weakly adhesion
6.	0.01	2	20	1 min @ 600 °C	Weakly adhesion
7.	0.01	5	10	1 min @ 200 °C	Appropriate
8.	0.01	5	20	1 min @ 200 °C	Appropriate
9.	0.01	5	10	1 min @ 400 °C	Weakly adhesion
10.	0.01	5	20	1 min @ 400 °C	Weakly adhesion
11.	0.01	5	10	1 min @ 600 °C	Weakly adhesion
12.	0.01	5	20	1 min @ 600 °C	Weakly adhesion
13.	0.01	10	10	1 min @ 200 °C	High thickness of GO film
14.	0.01	10	20	1 min @ 200 °C	High thickness of GO film
15.	0.01	10	10	1 min @ 400 °C	Delaminated GO film
16.	0.01	10	20	1 min @ 400 °C	Delaminated GO film
17.	0.01	10	10	1 min @ 600 °C	Delaminated GO film
18.	0.01	10	20	1 min @ 600 °C	Delaminated GO film
19.	0.01	20	10	1 min @ 200 °C	High thickness of GO film
20.	0.01	20	20	1 min @ 200 °C	High thickness of GO film
21.	0.01	20	10	1 min @ 400 °C	Delaminated GO film
22.	0.01	20	20	1 min @ 400 °C	Delaminated GO film
23.	0.01	20	10	1 min @ 600 °C	Delaminated GO film
24.	0.01	20	20	1 min @ 600 °C	Delaminated GO film
25.	0.01	30	10	1 min @ 200 °C	High thickness of GO film
26.	0.01	30	20	–	Risk of sparkle during EPD
27.	0.01	30	10	1 min @ 400 °C	Delaminated GO film
28.	0.01	30	20	–	Risk of sparkle during EPD
29.	0.01	30	10	1 min @ 600 °C	Delaminated GO film
30.	0.01	30	20	–	Risk of sparkle during EPD
31.	0.2	2	10	1 min @ 200 °C	Appropriate
32.	0.2	2	20	1 min @ 200 °C	Appropriate
33.	0.2	2	10	1 min @ 400 °C	Weakly adhesion
34.	0.2	2	20	1 min @ 400 °C	Weakly adhesion
35.	0.2	2	10	1 min @ 600 °C	Weakly adhesion
36.	0.2	2	20	1 min @ 600 °C	Weakly adhesion
37.	0.2	5	10	1 min @ 200 °C	Appropriate
38.	0.2	5	20	1 min @ 200 °C	Appropriate
39.	0.2	5	10	1 min @ 400 °C	Weakly adhesion
40.	0.2	5	20	1 min @ 400 °C	Weakly adhesion
41.	0.2	5	10	1 min @ 600 °C	Weakly adhesion
42.	0.2	5	20	1 min @ 600 °C	Weakly adhesion
43.	0.2	10	10	1 min @ 200 °C	High thickness of GO film
44.	0.2	10	20	1 min @ 200 °C	High thickness of GO film
45.	0.2	10	10	1 min @ 400 °C	Delaminated GO film
46.	0.2	10	20	1 min @ 400 °C	Delaminated GO film
47.	0.2	10	10	1 min @ 600 °C	Delaminated GO film
48.	0.2	10	20	1 min @ 600 °C	Delaminated GO film
49.	0.2	20	10	1 min @ 200 °C	High thickness of GO film
50.	0.2	20	20	1 min @ 200 °C	High thickness of GO film
51.	0.2	20	10	1 min @ 400 °C	Delaminated GO film
52.	0.2	20	20	1 min @ 400 °C	Delaminated GO film
53.	0.2	20	10	1 min @ 600 °C	Delaminated GO film
54.	0.2	20	20	1 min @ 600 °C	Delaminated GO film
55.	0.2	30	10	1 min @ 200 °C	High thickness of GO film
56.	0.2	30	20	–	Risk of sparkle during EPD
57.	0.2	30	10	1 min @ 400 °C	Delaminated GO film
58.	0.2	30	20	–	Risk of sparkle during EPD
59.	0.2	30	10	1 min @ 600 °C	Delaminated GO film
60.	0.2	30	20	–	Risk of sparkle during EPD

considered. According to the basically visual results of prepared samples (the results of right column of Table 3), the initial appropriate used conditions for electrophoretic deposition were shown in Table 4.

As it obvious some conditions resulted a film with weak adhesion properties such as runs of 2, 3, 4, 11 and 12, so is not suitable for future applications. On the other hand, by sharp increasing the application potential (up to 20 V), risk of sparkle formation on the anode is more increased such as runs of 26, 28, 30, 56, 58 and 60. Finally the best resulted runs of 1, 2, 7, 8, 31, 32, 37 and 38 seems the better conditions for further investigation called 0.01G-210, 0.01G-220, 0.01G-510, 0.01G-520, 0.2G-210, 0.2G-220, 0.2G-510, 0.2G-520 respectively.

The images of high thickness graphene film after thermal annealing in different temperatures (200, 400 & 600 °C) are shown in Fig. 3. As can be seen a dark black film formed on bare copper attributed to high thickness layers of GO so that it easily dislodge from the surface at higher temperatures.

Table 4
The characteristics of appropriate samples.

Sample code	GO conc. (%w/w)	Application voltage (V)	Application time (s)	Thermal annealing condition
0.01G-210	0.01	2	10	1 min @ 200 °C
0.01G-220	0.01	2	20	1 min @ 200 °C
0.01G-510	0.01	5	10	1 min @ 200 °C
0.01G-520	0.01	5	20	1 min @ 200 °C
0.2G-210	0.2	2	10	1 min @ 200 °C
0.2G-220	0.2	2	20	1 min @ 200 °C
0.2G-510	0.2	5	10	1 min @ 200 °C
0.2G-520	0.2	5	20	1 min @ 200 °C

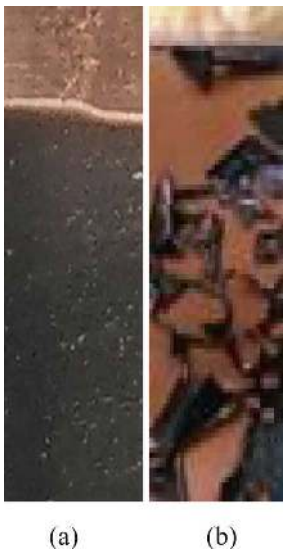

Fig. 3. Image of high thickness GO film (a: after thermal annealing at 200 °C, b: after thermal annealing at 400 °C).

After visually investigation the effects of GO concentration and electrical potential of EPD on deposition behavior of GO on copper foil, the application potentials of 2 and 5 V at application times of 10 and 20 s were selected for two concentrations of prepared GO suspensions. The characteristics of appropriate samples are introduced in Table 4.

3. Results and discussion

According to the structural model of GO (introduced by Gao et al. [31]) that shown in Fig. 4, the most functional groups of GO are hydroxyl (OH), carboxylic acid (COOH) and epoxy (COC) so that by stable suspension of GO in water and surface ionization of functional groups, the effective surface charge of this compound is negative. In the electrical field of EPD process, the GO is attracted to the positively charged surface (anode).

3.1. Characterization of GO

To establish that the commercial available GO used in this study had similar properties as previously reported, Raman spectroscopy and SEM were applied to characterized it. The Raman spectrum and SEM image of used GO are shown in Fig. 5.

Fig. 5 shows a typical Raman spectrum of used graphene oxide. The G peak is the result of in plane optical vibrations and has a literature value of 1580 cm^{-1} that matches approximately with obtained result (1600.8 cm^{-1}). The D peak is located at 1357.6 cm^{-1} and is due to first order resonance that matches with previous studies very well [32]. Plannar morphology of GO was investigated by SEM technique which were similar to previous reported [33]. All these results established that the GO used in this study was truly a single layer sheet.

Basically G and D- peaks of graphene/GO signifies sp^2 hybridization (graphitic signature of carbon) and disorder due to the defects induced on the sp^2 hybridized hexagonal sheet of the carbon respectively, range of G ~ 1500–1600 cm^{-1}/ range of D ~ 1300–1400 cm^{-1}.

In the case of GO the intensity and line-width of D is larger than G indicates the more disorder due to defects from strong treatment with chemicals, and amorphous carbon content will be more (1300–1450 cm^{-1}) i.e. sp^3 cluster is more than sp^2. Peak from 2650–2700 called 2nd order disorder mode (2D) for carbon nano material. In the case of graphene it is not due to the disorder significant for double resonance of scattered photons by excitation wavelength and signature for the layer number, area and quality of the graphene intensity of the 2D should be more than G.

3.2. Characterization of electrodeposited graphene films

EPD of dispersed GO on copper substrate was done based on the best conditions of applied potential, time and annealing temperatures (Table 5). Images of appropriate samples after thermal annealing are shown in Fig. 6.

Visual results showed a remarkable darkness by increasing the GO concentrations in the same applied potentials (samples of a-1 and c-1 and also b-1 and d-1 from Fig. 6). The effect of higher application time on darkness of films is obvious at samples of c-1 and c-2 and also d-1 and d-2. As the same as GO concentration, applied potential and time of applied EPD were affected on thickness of GO layers certainly.

Thermal annealing procedure is found only to produce small size and wrinkled graphene sheets from graphite or reduced graphene oxide (RGO) from graphene oxide (GO) only in optimized temperatures. This is mainly because the decomposition of oxygen-containing groups also removes carbon atoms from the carbon plane. A notable effect of thermal exfoliation is the structural damage to graphene sheets caused by the release of carbon dioxide in high temperatures. Approximately 30% of the mass of the graphite oxide is lost during the exfoliation process, leaving behind lattice defects throughout the sheet. Defects inevitably affect the electronic properties of the product by decreasing

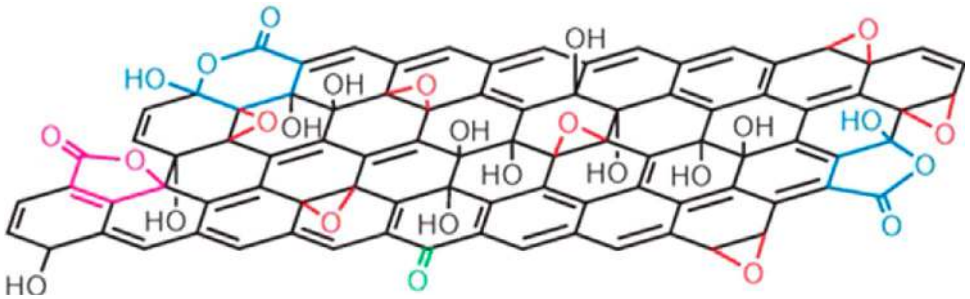

Fig. 4. The structural model of GO.

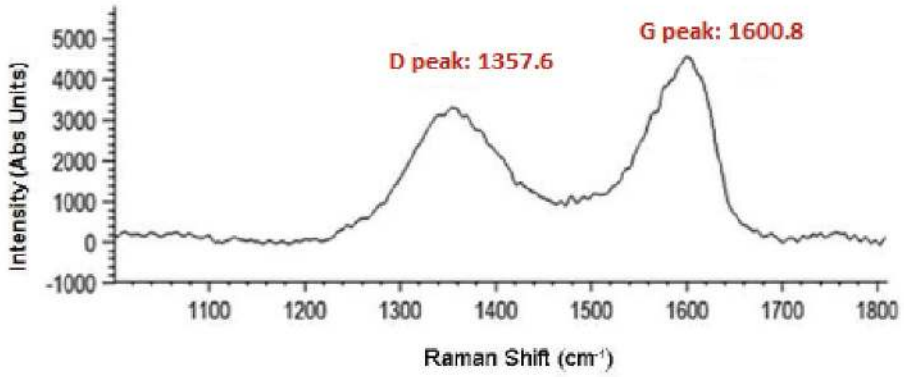

(a)

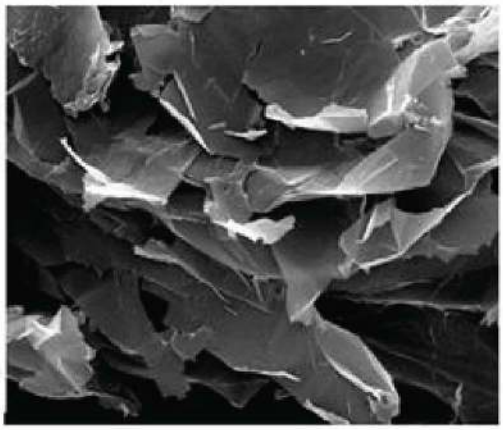

(b)

Fig. 5. (a) Raman spectrum at λ = 532 nm and (b) SEM image of used GO.

Table 5
The highlighted zones of FTIR diagram.

compound exponent	Zone number	ν (cm^{-1})	Functional group
GO exponent (Oxygen groups)	2	1725	(C = O) Carboxyl/ Carbonyl
	4	1407	(C = O) Carboxyl
	5	1225	(COC) Epoxy
	6	1057	(C−O) Alkoxy
RGO exponent	1	3200	(C−H) Aromatic ring
	3	1618	(C = C) Aromatic ring

the ballistic transport path length and introducing scattering centers [34]. In this study, we found the optimized temperatures for thermal annealing of deposited GO films in [1 min @ 200 °C].

In cases where the thickness of graphene film has increased, with the temperature increase due to the thermal stress, adhesion of the graphene film to the substrate was greatly reduced.

In order to evaluate the effect of variables of applied potential, time and GO solution concentration on EPD characterizations of prepared films, the electrical current behavior, deposition efficiency, sheet resistance, surface morphology, functional groups and film thickness were investigated by current density and deposition efficiency analysis, Ohm resistance measurement, SEM, FTIR and AFM techniques and discussed as followed. Also to punctual analyze the chemical structure of obtained annealed graphene film, XRD pattern, UV–Vis absorption spectrum and TGA behavior are investigated.

While GO suspension concentration decreases, the GO sheet concentration is decreased too, where the sheet resistance decreases too. It is reasoned that when the suspension concentration is decreased, the number of oxygen atoms adsorbed on the thin film will be increased, causing a decrease of the defect density and resulting in a decrease of the sheet concentration. These results imply that as the suspension concentration is decreased, the thin films come closer to the stoichiometrical composition and the Hall mobility is increased. It is reasoned that Hall mobility is more affected by the quality enhancement of the thin film than by the change in its resistance. Transmittance and sheet resistance decreased with increasing film thickness (but sheet resistance has an optimum point so after that because of graphene site aggregation, the sheet resistance increased by increasing the GO thickness/see the results of Table 6). In this study, the GO suspension concentration of 0.01% (by weight) resulted in lower thickness and more electrical conductivity. The results of this study confirms the results of Chowdhurry et al. [35].

For evaluation the direct effect of electrical potential on the deposition behavior of GO, the electrical current density was monitored during potential application (at steps of 2, 5, 10, 20 and 30 V). The results of electrical current behavior of electrodeposited samples during

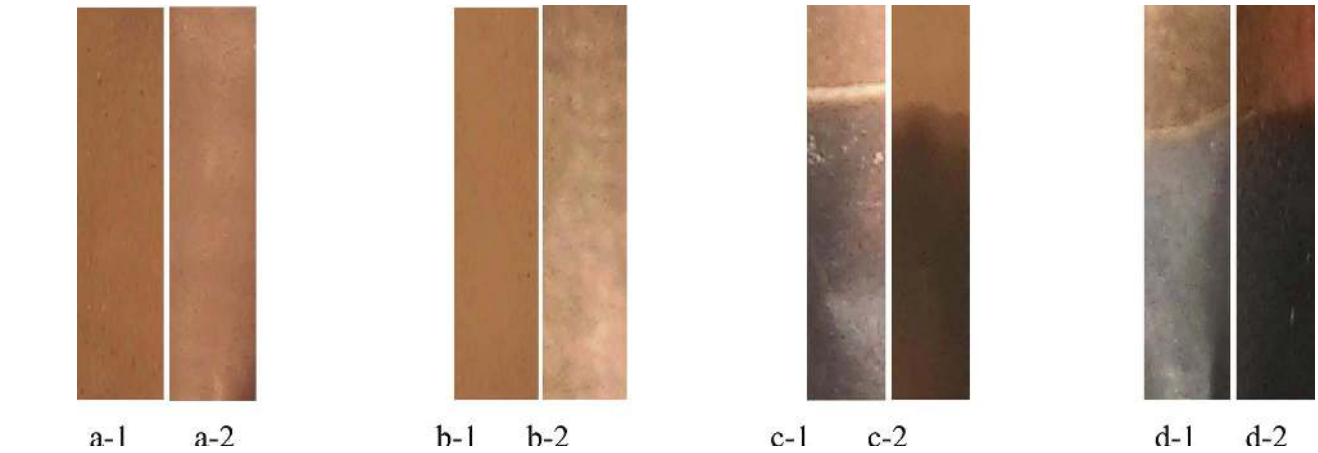

Fig. 6. Images of prepared samples after thermal annealing (a-1:0.01G-210, a-2:0.01G-510, b-1:0.01G-510, b-2:0.01G-520, c-1:0.2G-210, c-2:0.2G-220, d-1:0.2G-510, d-2:0.2G-520).

Table 6
Electrodeposion characteristics of prepared samples.

Sample code	Deposition efficiency ($mg.cm^{-2}$)	Sheet resistance (K Ω)/[sheet resistance of bare copper: 2.40 KΩ]	Average thickness of GO layers (nm)/ [evaluated by AFM method]
0.01G-210	0.11	0.81	5.4
0.01G-220	0.15	0.84	13.6
0.01G-510	0.22	0.91	15.6
0.01G-520	0.26	0.92	25.5
0.2G-210	0.50	2.11	50.0
0.2G-220	0.75	2.20	58.3
0.2G-510	0.91	2.71	70.6
0.2G-520	1.21	2.83	95.7

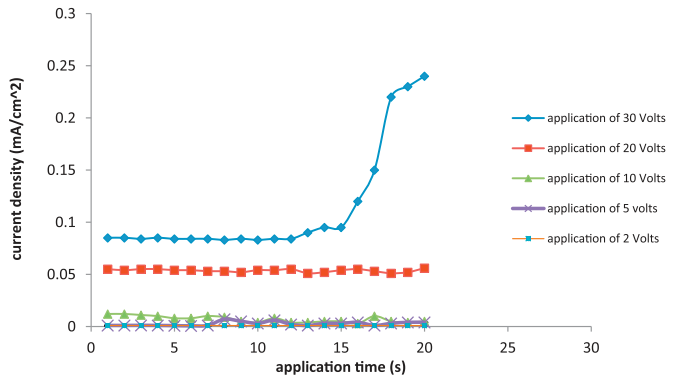

Fig. 7. The results of electrical current behavior of electrodeposited samples during potential application.

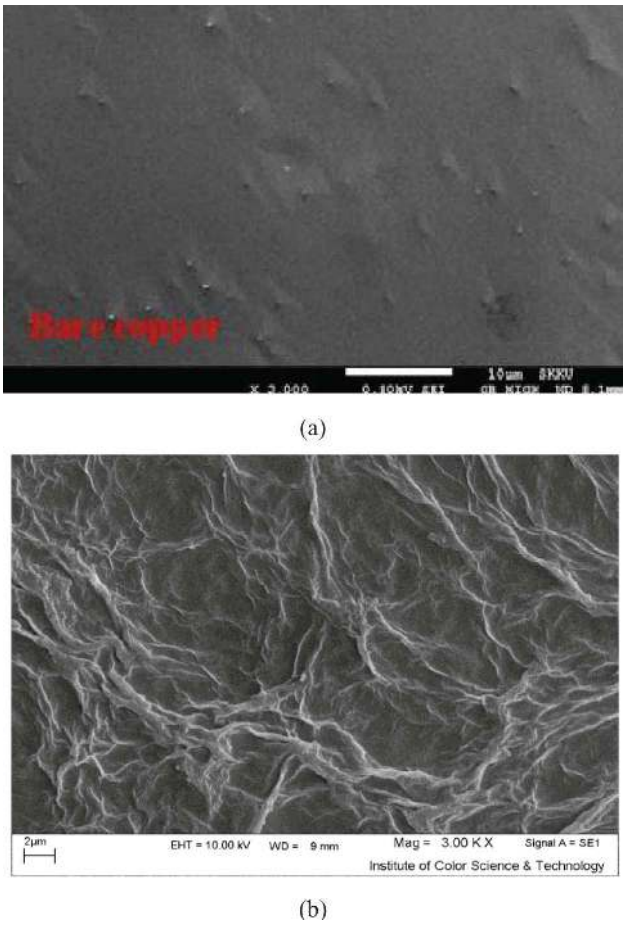

Fig. 8. The images of SEM of a) bare copper foil and b) GO electrocoated sample (0.01G-210).

potential application is shown in Fig. 7.

According to the results of Fig. 6, during the electrophoretic deposition of GO on the copper foil, because of high conductivity of the copper foil, the changes of electrical current at application potentials of 2, 5, 10 and 20 V are approximately constant. On the other hand, because of very low thickness of copper foil (~40 μm) at application potential of 30 V, the sparkle was seen at the copper substrate in application times of more than 10 s. Also, thickness of the GO film got very high and the electrical current density was increased significantly in this condition. Therefore, electrical potentials of more than 20 V is not suggested for application of GO film on the copper substrate.

To investigate the deposition efficiency of electrocoated films, 1 cm^2 of the bare copper substrate and GO coated surface were isolated. Weight of the bare copper foil was measured before and after EPD and thermal annealing of the electrocoated samples, so the weight of the isolated GO coated samples were obtained. The results of deposition efficiency of electrocoated samples are shown in Table 6. According to the results of Table 6, by increasing the applied potential of EPD, the deposition efficiency of GO film on the copper substrate is increased

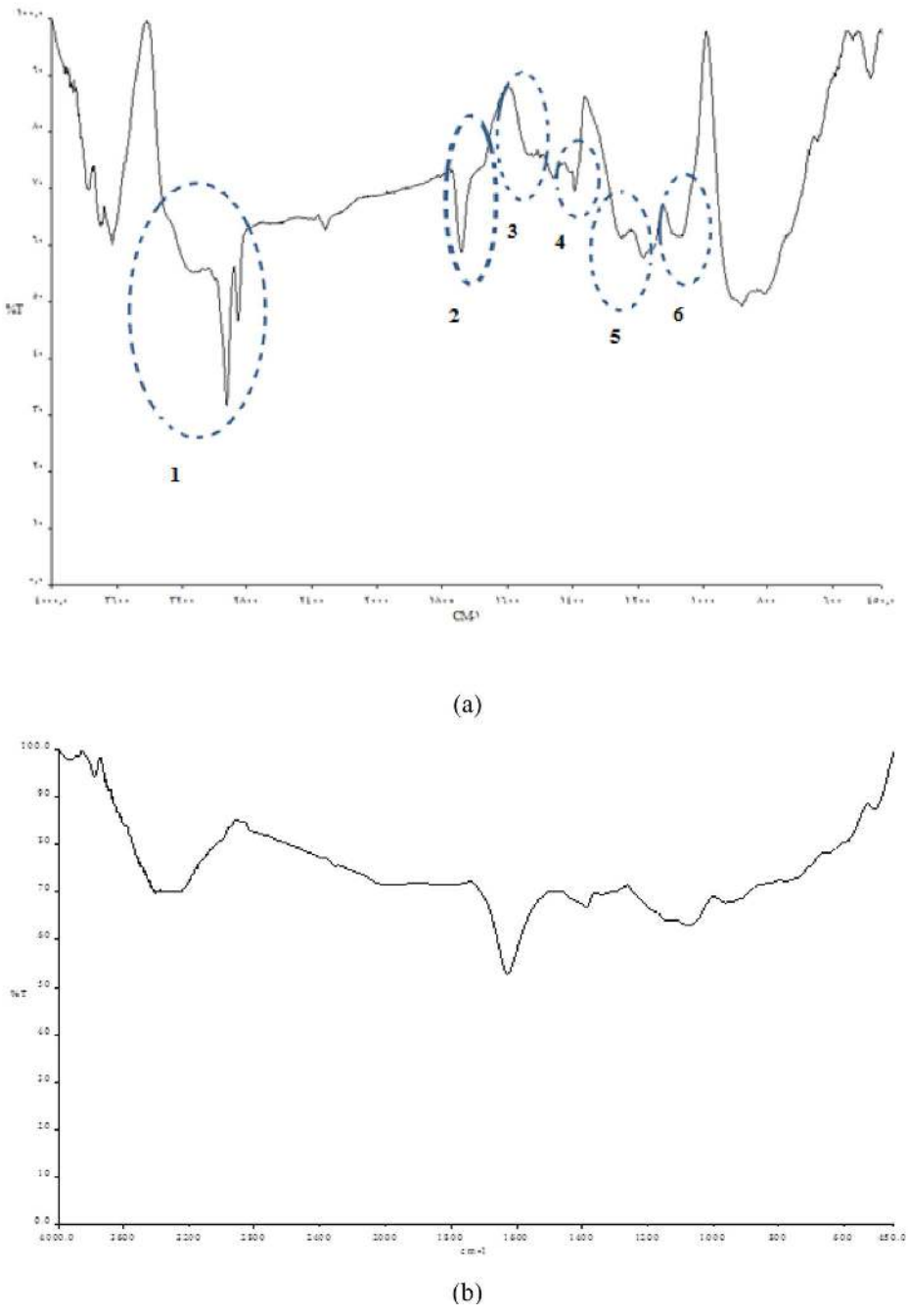

Fig. 9. a: FTIR results of stable GO suspension (0.2 by weight), b: thermally annealed GO film on the copper substrate.

continually. This result confirms increasing the number of deposited film layers on the copper surface in these conditions. The remarkable point is that the concentration of GO suspension effect on the increasing the deposition efficiency and thickness of GO layers is more evident in compared to the applied potential and application time effects.

The images of scanning electron microscopy (SEM) of bare copper foil and GO electrocoated sample (0.01G-210) are shown in Fig. 8.

As it is seen clearly in Fig. 8, the wrinkled graphene layers are deposited on the copper surface completely uniform.

FTIR measurements was carried out in order to confirm the GO and RGO formation during EPD and thermal annealing of samples. FTIR results of stable GO suspension (0.2 by weight) and thermally annealed GO film on the copper substrate (0.2G-520) are shown in Fig. 9.

According to the FTIR diagrams of Fig. 9, the highlighted zones of diagram (a) are introduced in Table 5.

The FTIR results manifested that the presence of groups containing oxygen in graphene compound of thermally annealed samples are reduced significantly that it confirms sufficient thermal reduction of graphene oxide and achieving reduced graphene oxide (RGO) in these conditions.

To confirm the RGO obtain after thermal annealing, XRD pattern and UV–Vis. absorption spectra of reduced graphene oxide film are discussed as below.

XRD patterns of powdered graphene oxide and annealed

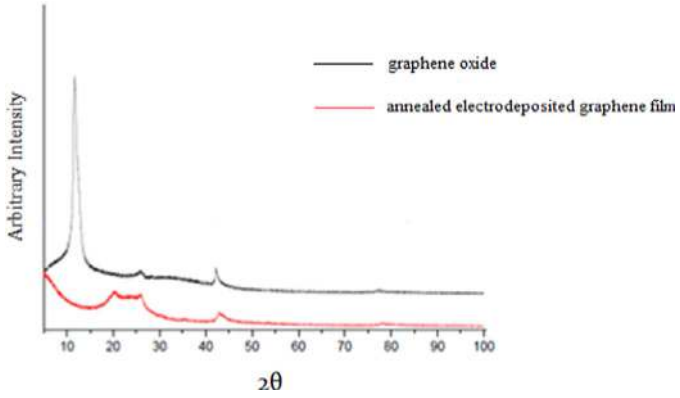

Fig. 10. XRD patterns of powdered graphene oxide and annealed electrodeposited graphene film (monochromatic CuKα radiation (λ = 1.5406 A°) with scan rate of 0.1° min^{-1}).

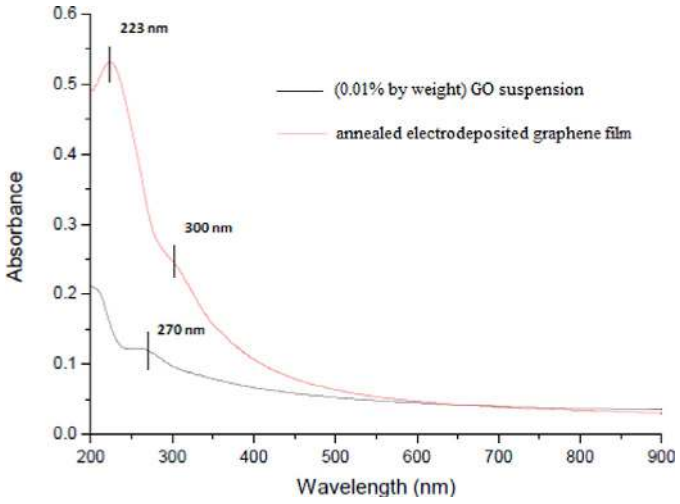

Fig. 11. UV–Vis absorption spectrum of (0.01% w/w) GO suspension and annealed electrodeposited graphene film.

electrodeposited graphene film are shown in Fig. 10.

In the XRD pattern of graphene oxide (powder), the strong and sharp peak at 2θ = 11.7° corresponds to an interlayer distance of 7.6 Å (d002). Annealed electrodeposited graphene film (RGO) shows a broad peak that can be fitted by using a Lorentzian function into three peaks centered at 2θ = 20.17°, 23,78° and 25.88°, corresponding to interlayer distances of 4.47, 3.82 and 3.53 Å, respectively. These XRD results are related to the exfoliation and reduction processes of GO and the processes of removing intercalated water molecules and the oxide groups during thermal annealing of electrodeposited graphene films.

The samples of (0.01% w/w) GO aqueous suspension before electrodeposition process and annealed electrodeposited graphene film were determined by UV–Vis absorption spectrum. The results of UV–Vis absorption spectra are shown in Fig. 11.

The UV–Vis spectra of GO exhibits a maximum absorption peak at about 223 nm, corresponding to π-π* transition of aromatic C—C bonds and a shoulder around 300 nm due to the n-π* transition of C = O bonds. The absorption peak for reduced GO had red shifted to 270 nm. This phenomenon of red shift has been used as a monitoring tool for the reduction of GO.

One of the most important characterizations of graphene sheets is their high electron transfer rate. In order to investigate the conductivity of prepared GO films, the sheet resistance (R_{sh}) of graphene EPDs were compared with that of bare copper. The results of sheet resistance measurement of samples are listed in Table 6.

The results showed that the sheet resistance of the copper substrate with less-layered graphene coating (0.01G-210) is decreased to a third of initial value of un-coated copper surface sheet resistance. In other words, the electrical conductivity of electrocoated copper surface after thermal annealing (in accordance with the application conditions of sample# 0.01G-210) is increased three times. According to the results of Fig. 8, by increasing the thickness of RGO coating (by increasing the GO concentration, electrical potential or application time), the sheet resistance of RGO is increased continually so that by increasing the GO concentration, the rate of sheet resistance increasing trend is much faster. As it is clear from the Fig. 8, the minimum sheet resistance of electrodeposited graphene film was 0.8 KΩ (sample#0.01G-210) compared to the maximum one (2.8 KΩ). The reason of this fact is thickness increase of the GO layers deposited on the copper surface and aggregation of graphene sites on the copper surface. In this condition, by significantly increase in thickness of graphene layers, the more resistance barrier is created in the way of electron transfers, so theoretical adaptation of electron mobility within the mono-layer graphene is less according to the Dirac equation.

The sheet resistance reported by Rana and coworkers [26] for electrochemically reduced graphene oxide and vacuum-filter reduced graphene oxide is 2.4 and 43 KΩ respectively so that the sheet resistance of graphene film that prepared by the method of this research work is lower than many other research works. Thickness of EPD GO layers were determined based on AFM data.

The images of atomic force microscopy (AFM) of samples are shown in Fig. 12.

The average thickness of GO layers that applied on the copper surface is evaluated and the results are shown in Table 6.

The results of AFM showed that the minimum average thickness of electrodeposited graphene film was 5.44 nm (sample#0.01G-210) compared to the maximum average that was 95.7 nm (sample#0.2G-520). The AFM data manifested that by increasing the key parameters of EPD (GO concentration, electrical potential and application time), the average thickness of GO layers deposited on the copper surface is increased continually. Also, by increasing the thickness of GO layers, the coarseness profile of samples is much greater, so it confirms the increasing of the wrinkling of GO layers too.

4. Conclusion

In this research work, anodic electrodeposition of stable graphene oxide (GO) suspension was done on bare copper foil. The key parameters of EPD process (concentration of GO suspension, electrical potential and application time) due to the better morphology and electrical conductivity and minimum thickness of electrodeposited GO layers were optimized. Electrical current behavior, deposition efficiency, FTIR spectroscopy, sheet resistance measurement, scaning electron and atomic force microscopy tests were evaluated on the prepared electrocoated GO films applied on copper substrate. All of the carried tests showed that by increasing the key parameters of EPD, the average thickness of electrodeposited GO layers are increased continually so that the GO concentration effect is the most evident factor. In this study the minimum sheet resistance and average thickness of electrodeposited RGO layers with uniform wrinkled morphology are achieved at EPD conditions of 2 V in 10 s and annealed at 200 °C for 1 min. In these conditions, the minimum sheet resistance and average thickness of electrodeposited graphene films achieved that are 0.8 KΩ and 5.44 nm respectively. The results of this research manifested that the EPD method is the novel, low cost and well controllable method to fabricate very conductive electrode base for electro-optical devices that this method could be replaced by chemical vapor deposition technique to form a low thickness GO film very well.

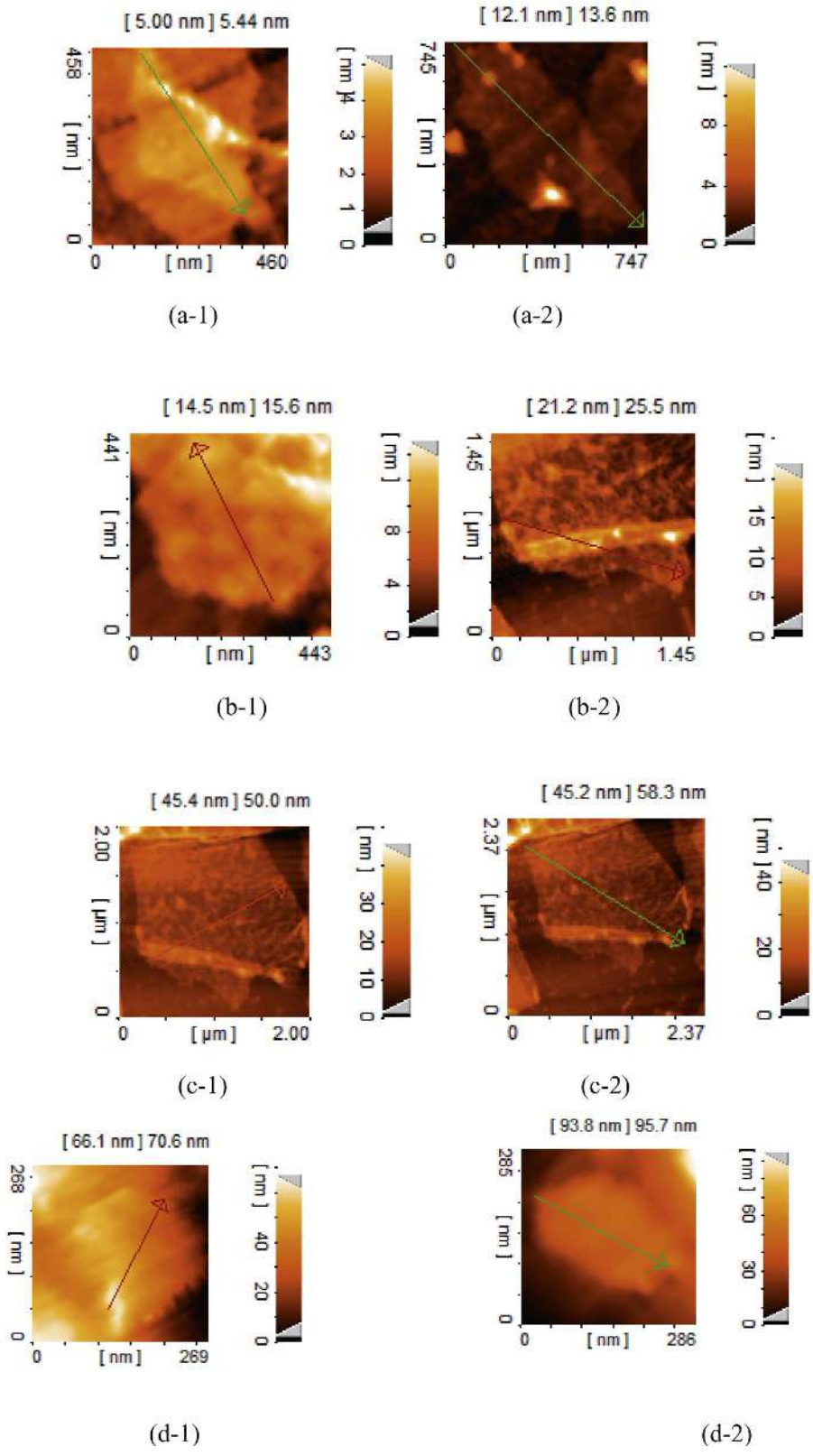

Fig. 12. Images of AFM of samples (a-1:0.01G-210, a-2:0.01G-220, b-1:0.01G-510, b-2:0.01G-520, c-1:0.2G-210, c-2:0.2G-220, d-1:0.2G-510, d-2:0.2G-520).

Acknowledgments

We would like to thank the Center of Excellence for Color Science and Technology(CECST), Institute for Color Science and Technology, Tehran-Iran for providing us a good environment and facilities to complete this project.

References

[1] M. Sima, I. Enculescu, A. Sima, Synthesis and characterization of glass doped reduced graphene oxide, Optoelectron. Adv. Mater. 5 (2011) 414–418.
[2] Q. Mei, K. Zhang, Highly efficient photoluminescent graphene oxide with tunable surface properties, Chem.Commun. 46 (2010) 7319–7321.
[3] Y. Pang, Y. Cui, Fluorescence quenching of organic dye by graphene: interaction and its mechanism, Micro Nanolett. 7 (2012) 608–612.
[4] H. Kautsky, Quenching of luminescence by oxygen, Trans. Faraday Soc. 35 (1939) 216–219.
[5] K. Fan, Z. Guo, How graphene oxide quenches fluorescence of Rhodamine 6 G, Chin. Phys. Soc. 3 (2013) 252–258.
[6] H.S. Ramakrishna, K.S. Subrahmanyam, Quenching of fluorescence of aromatic molecules by graphene due to electron transfer, Micro Nanolett. 45 (2013) 452–468.
[7] Y. Liu, Investigation on fluorescence quenching of dyes by graphite oxide and graphene, Appl. Surf. Sci. 257 (2011) 5513–5518.
[8] M. Ghazinejad, H. Hosseini, J. Reiber Kyle, Fluorescence quenching metrology of Graphene, Photonic and Phononic Properties of Engineered Nanostructures, 8994 2015, pp. 277–285.
[9] M.V. Encinas, E.A. Lissi, Intermolcular quenching of 2,3-dimethylnaphthalene fluorescence by peroxidesmand hydroperoxides, Photochem. Photobiol. 37 (1983) 251–255.
[10] M.R. Eftink, Fluorescence Quenching: Theory And Applications, Lakowicz Plenum Press, NewYork, 1991, pp. 53–126.
[11] A.S. Holmes, Fluorescent quenching by metal ions in lipid biology, Biophys. Chem. 48 (1993) 193–204.
[12] D. Daems, N. Boens, fluorescence quenching with lindone indone, Eur. Biophys. 17 (1989) 25–36.
[13] R.F. Jones, Quenching of naphthalene luminescence by oxygen and nitric oxide, J. Chem. Phys. 54 (1971) 3360–3366.
[14] R.F. Steiner, E.P. Kirby, The interaction of the groun and excited states of indole derivative with electron scavengers, J. Chem. Phys. 73 (1969) 4130–4135.
[15] R.S. Swathi, K.L. Sebastian, long range resonance energy transfer from a dye molecule to graphene has (distance)$^{-4}$ dependence, J. Chem. Phys. 130 (2009) 86101–86109.
[16] R.S. Swathi, K.L. Sebastian, Resonance energy transfer from a dye to graphene, J.Chem.Phys. (2008) 129.
[17] P.O. Huang, J. Liu, DNA-length-dependent fluorescent signaling on graphene oxide surface, Small 8 (2012) 977–983.
[18] J. Kim, L.J. Cote, Visualizing graphene based sheets by fluorescence quenching microscopy, J. Chem. Phys 132 (2010) 260–267.
[19] X. Wang, Ultrasensitive and selective detection of a prognostic indicator in early stage cancer using graphene oxide and carbon nanotube, Adv. Funct. Mat. 20 (2010) 3967–3973.
[20] X. Zhu, Y. Shen, Detection of microRNA by using reduced graphene oxide, Chem.Common. 51 (2015) 10002–10005.
[21] J. Balapanuru, J.X. Yang, A graphene oxide-organic dye ionic complex with DNA sensing and optical limiting properties, Angew. Chem. 49 (2010) 6549–6553.
[22] Y. Zhau, X. Gang, Review on the graphene based optical fiber chemical and biological sensor, Sensors Actuators B 231 (2016) 324–340.
[23] S. Lajevardi Esfahani, Z. Ranjbar, S. Rastegar, An electrochemical and mechanical approach to the corrosion resistance of cathodic electrocoatings under combined cyclic and DC polarization conditions, Prog. Org. Coat. 77 (2014) 1264–1270.
[24] S. Lajevardi Esfahani, Z. Ranjbar, S. Rastegar, Investigation of protective behavior of different cathodic electrocoatings using different anti-corrosive tests (modified AC/DC/AC test, EIS and salt spray), J. Color. Sci. Tech. 8 (2013) 119.
[25] S. Lajevardi Esfahani, Z. Ranjbar, S. Rastegar, Evaluation of anticorrosion behavior of automotive electrocoating primers by the AC-DC-AC accelerated test method, J. Prog. Color Colorants Coat. 7 (2014) 187.
[26] K. Rana, J. Singh, J.H. Ahn, A graphene-based transparent electrode for use in flexible optoelectronic devices, J. Mater. Chem. C 2 (2014) 2646–2656.
[27] S. Seraj, Z. Ranjbar, A. Jannesari, Synthesis and characterization of an anticratering agent based on APTES for cathodic electrocoatings, Prog. Org. Coat. 77 (2014) 1735–1740.
[28] D. Joseph, R.M. Ilhan, A. Aksay, Graphene materials and their use in dye-sensitized solar cells, Chem. Rev. 114 (2014) 6323–6348.
[29] K. Rana, J. Singh, J.H. Ahn, A graphene-based transparent electrode for use in flexible optoelectronic devices, J. Mater. Chem. C 2 (2014) 2646–2656.
[30] E. Morales-Narvaez, A. Merkoci, Graphene oxide as an optical biosensing Platform, Adv. Mater. 24 (2012) 3298–3308.
[31] W. Gao, L.B. Alemany, L.J. Ci, P.M. Ajayan, New insights into the structure and reduction of graphite oxide, Nat. Chem. 1 (2009) 403–408.
[32] D. Yang, A. Velamakanni, G. Bozoklu, S. Park, M. Stoller, R.D. Piner, S. Stankovich, I. Jung, D.A. Field, C.A. Ventrice, S. Ruoff, Chemical analysis of graphene oxide films after heat and chemical treatments by X-ray photoelectron and micro-Raman spectroscopy, Carbon 47 (2009) 145–152.
[33] C. Fu, G. Zhao, H. Zhang, S. Li, Evaluation and characterization of reduced graphene oxide nanosheets as anode materials for lithium-ion batteries, Int. J. Electrochem. Sci. 8 (2013) 6269–6280.
[34] S. Pei, H.M. Cheng, The reduction of graphene oxide, Carbon (2011), http://dx.doi.org/10.1016/j.carbon.2011.11.010.
[35] F.A. Chowdhurry, T. Morisaki, J. Otsuki, M.S. Alam, Appl. Nanosci. 6 (2013) 477–483.